

Flow and Tilt-Induced Orientation of the Moving Vortex Lattice in Amorphous NbGe Superconducting Thin Films

Nobuhito KOKUBO^{1*}, Tetsuya YOSHIMURA², and Bunjyu SHINOZAKI²

¹*Department of Engineering Science, The University of Electro-Communication, Tokyo 182-8585, Japan*

²*Department of Physics, Kyushu University, Fukuoka 812-8581, Japan*

The orientation and deformation of moving vortex lattices in the flux-flow state have been investigated in amorphous superconducting NbGe thin films. Employing a mode-locking technique, we detect how moving lattices deform and their orientation changes as a magnetic field is tilted from normal to the film surface. For high tilt angles the lattice orientation is aligned parallelly with the tilt direction. Meanwhile for low tilt angles the lattice orientation depends on the vortex velocity and a velocity-induced reorientation occurs. The characteristic velocity for the reorientation varies remarkably as the moving lattices deform. The observed features are consistent with an extended bond-fluctuation theory, revealing that the anisotropic shaking vortex motion is essential for determining the orientation of moving vortex lattices.

KEYWORDS: vortex lattice, reorientation, mode locking, flux flow, amorphous superconductor

1. Introduction

Over the past few decades there has been considerable interest in the orientation of a hexagonal vortex lattice (VL) in type II superconductors.¹⁾ Within the London approximation for isotropic superconductors all the possible orientations of the vortex lattice are degenerate in energy,^{2,3)} while this is lifted not simply by tilting an applied magnetic field,^{4,5)} but also when driven by applying a transport current. In experiments various imaging techniques such as Bitter decoration,⁶⁾ small angled neutron scattering^{7,8)} and scanning tunneling microscopy⁹⁻¹¹⁾ have provided structural evidence for the hexagonal order in moving VLs, and some of them have shown that the lattice orientation (one of close-packed directions of the hexagonal VL) is aligned to be either parallel or perpendicular to the flow direction. These flow-induced orientations, including a reorientation between them, have been observed on both crystalline^{6,10)} and non-crystalline weak pinning superconductors,¹²⁻¹⁴⁾ and thus underlying crystallographic orientations are not at play. It is rather essential to understand how quenched disorder affects the orientation of moving VLs. Schmid and Hauger pointed out, for a long time ago, that the dissipation of the vortex motion is minimized when the lattice orientation is aligned parallelly with the direction of its motion.¹⁵⁾ The parallel orientation has been supported by recent theoretical and numerical simulation studies¹⁶⁻¹⁸⁾ including the unique concept of the shaking temperature quantifying the effective influence of inhomogeneous environment on moving vortices.¹⁹⁻²¹⁾ However, the other lattice orientation, the perpendicular orientation, has been shown in limited theoretical studies with different approaches.²²⁻²⁴⁾ Therefore, it needs a physical picture which describes fully the puzzling mechanism for those two orientations, including the reorientation of moving VLs.

The issue of the orientation of moving VLs would be interesting when the magnetic field is rotated from normal to the sample surface. Since the orientation of moving lattices should be aligned parallelly with the tilt direction,³⁾ one expects that the tilt-induced mechanism competes with the flow-induced one when tilt- and flow-induced orientations are dif-

ferent. In addition, for thin superconductors, the field inclination leads to the deformation of VLs in the sample surface frame.²⁵⁾ Our principle interest is to what extent the lattice deformation (the anisotropy in VL parameters) could bear upon the reorientation of moving lattices. To address the issue, in this study, we present the flow- and tilt-induced (re)orientation of (deformed) moving vortex lattices observed on weak pinning, amorphous NbGe superconducting thin films by means of a mode-locking (ML) technique.

This manuscript is organized as follows: In Sec. 2 we describe sample preparation and characterizations, followed by our experimental setup for ML measurements. In Sec. 3 we present the experimental results of ML features and discuss the lattice orientation and the anisotropy in VL parameters obtained in different tilt directions. Derived consequences for dynamic phase diagrams of the lattice orientation are discussed and they are compared with an extended anisotropic bond-fluctuation theory.^{21,26)} Finally, we summarize our findings in Sec. 4.

2. Experimental

Amorphous Nb_xGe_{1-x} ($x \approx 78\%$) superconducting thin films were deposited upon Si substrates by rf magnetron sputtering. We used a 3 inch diameter niobium target (purity 99.95%) with germanium sheets (purity 99.999%) on top and applied 70 W rf power to the target. The NbGe films with 0.28 μm thick were structured into bridge patterns by using metal masks covering Si substrates. We used two bridge films of which geometry and material parameters are as follows: For the film 1 the width w and length l between voltage contacts are 0.10 mm and 4.00 mm, respectively; the superconducting transition temperature T_c is 4.09 K, the slope S of the second critical field B_{c2} against temperature T near T_c is ≈ 2.1 T/K, and the normal state resistivity ρ_n is 1.44 $\mu\Omega\text{m}$. Using the dirty-limit expression,²⁷⁾ the coherence length $\xi(0)(= 1.81 \times 10^{-8} / \sqrt{ST_c})$ at $T = 0$ K is 6.1 nm, the penetration depth $\lambda(0)(= 1.05 \times 10^{-8} \sqrt{\rho_n T_c^{-1}})$ at $T = 0$ K is 0.62 μm ($\gg \xi(0)$), and the Ginzburg-Landau parameter $\kappa(= 3.54 \times 10^4 \sqrt{S\rho_n})$ is 62. For the film 2 $w = 0.20$ mm, $l = 1.90$ mm, $T_c = 3.50$ K, $S \approx 2.0$ T/K, $\rho_n = 1.46 \mu\Omega\text{m}$, $\xi(0) = 6.9$ nm, $\lambda(0) = 0.68 \mu\text{m}$

and $\kappa = 68$. Because of large κ , the vortex density B is nearly equal to the applied magnetic field B_a (i.e., $B \cong B_a$) when the field is applied perpendicularly to the film surface.

The NbGe thin films have weak pinning properties for vortices in magnetic fields and temperatures studied. The depinning current density J_c determined from a current-voltage ($I-V$) curve with $1 \mu\text{V}$ criterion is typically $\sim 10 - 100 \text{ A/cm}^2$ at $T/T_c = 0.6$ and $B/B_{c2} = 0.4$, which is of the order of J_c for weak pinning, thin crystals of NbSe₂.²⁸⁾ The pinning strength can be characterized by the transverse correlation length R_c being roughly 10 times larger than the lattice spacing a_Δ of the regular hexagonal VL, determined from two-dimensional collective pinning analysis.^{27,29)} The $I-V$ curve exhibits the linear flux-flow behavior, of which flow resistivity was well discussed in Ref. 30.

We used a laboratory-built insert with a single-axis tilt stage. The film(s) and the tilt stage were immersed into pumped liquid ⁴He bath, of which vapor pressure was regulated by a throttle valve and a capacitance manometer. This allows us to precisely control the temperature of the bath from 4.2 K down to ~ 2 K.

A sketch in Fig. 1e represents the orientation of the magnetic field with respect to the film lying on the xy plane (the tilt stage). The transport current I is applied along the y axis and vortices flow along the x axis. θ is the tilt angle of the magnetic field from normal to the film surface (the z axis), and ϕ is the in-plane angle between the flow direction (the x axis) and the field projection onto the xy plane. In our experimental setup, θ was adjusted by rotating the tilt stage, and it was measured *in situ* with a Hall probe attached to the tilt stage (the xy plane). Due to the line tension of coaxial cables fixed onto the tilt stage, θ was varied within a limited range of $0^\circ \lesssim \theta \lesssim 70^\circ$. By contrast, the direction of the tilt plane was adjusted by rotating the bridge film about the tilt axis of the stage before cooling, and two directions of $\phi \approx 0^\circ$ and 90° were studied in the present study.

The mode locking is based on dynamic resonance, which occurs when an internal frequency $f_{int} = qv/a$, characterizing the periodicity (velocity modulation) of moving lattices in the flow direction, is related harmonically to the frequency f of an ac current I_{ac} superimposed on top of the transport (dc) current I , i.e., $qv/a = pf$, where v is the average velocity and p, q are integers.³¹⁻³⁸⁾ This technique allows us detect not only the periodic vortex spacing a along the flow direction, but also the deformation and orientation of moving VLs.¹²⁾ It has been shown that the large amplitude ac current ($I_{ac} \gtrsim I$) changes the orientation of moving lattices.³⁹⁾ In order to avoid this effect, in this study, we employ the rf impedance technique which can detect the mode locking with the *small* amplitude ac current ($I_{ac} \ll I$).^{13,31,40)} For the technique we used an LCR meter (Agilent 4285A) with dc bias option (4285A-001), allowing rf impedance measurements up to 30 MHz after careful calibration for the coaxial cables. All the measurements were performed after cooling the films in zero magnetic field.

3. Results and Discussion

3.1 Moving vortex lattices in a perpendicular magnetic field

To provide the physical picture(s) of the mode locking for moving VLs, let us show some of ML results observed in the flux-flow state for the magnetic field applied perpendicularly

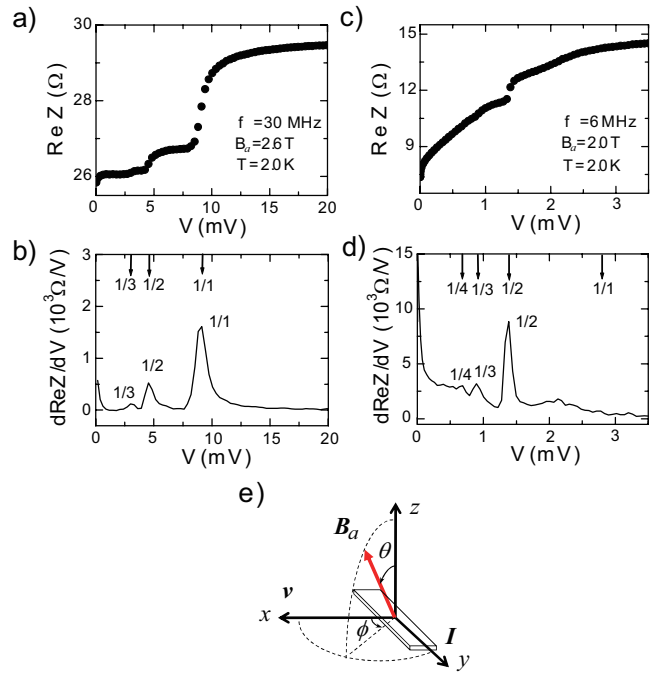


Fig. 1. (Color online) Mode-locking features observed in the film 1 at 2.0 K. (a) The real part ReZ of rf impedance vs. voltage V observed at 30 MHz and 2.6 T. The result at 6 MHz and 2.0 T is given in (c). The derivative curves of (a) and (c) are shown in (b) and (d), respectively. Arrows in (b) and (d) indicate fundamental and subharmonic ML voltages. (e) Schematic representation of the orientation of the applied magnetic field B_a with respect to the film (the xy plane). The directions of the vortex flow v and the transport current I are indicated. θ defines the tilt angle of the applied magnetic field B_a with respect to normal to the sample surface (the z axis). The tilt plane in which B_a rotates is characterized by the in-plane angle ϕ between the flow direction and the field projection on to the film surface.

we ramped up/down dc current, with superimposing the small, constant amplitude of ac current on top:⁴⁰⁾ As responses, we measured both the flux-flow (dc) voltage V and the real part ReZ of the complex rf impedance. To display how the complex impedance shows a ML feature(s), we plot ReZ against V . The plot thus obtained in the film 1 is shown in Fig. 1a. One can see that ReZ exhibits multiple jumps, as observed in previous studies.^{13,31)} The ML feature can be more clearly displayed by plotting the derivative of the $ReZ - V$ curve in Fig. 1b, where multiple peaks of $dReZ/dV$ are visible. These can be identified with the fundamental ($p/q = 1/1$) and subharmonics ($p = 1, q > 1$) using the following arguments: the $dReZ/dV - V$ curve has three peaks with different height. Focusing on the corresponding voltages for the peaks, one can find that the voltage for the largest peak is nearly two (three) times larger than one for the second largest peak (the smallest peak). Consequently, we find that the largest peak corresponds to fundamental, and the second and third ones are subharmonics of $p/q = 1/2$ and $1/3$, respectively. No harmonic with $p \geq 2$ appears because of the small amplitude ac current.^{41,42)} Another $ReZ - V$ curve is shown in Fig. 1c. The differential plot of the $ReZ - V$ curve (Fig. 1d) shows clearly that the largest and second largest peaks correspond to $1/2$ and $1/3$ subharmonics, respectively. The smallest peak is $1/4$ subharmonic, and the fundamental peak is not visible. Those two sets of the ML features with the fundamental largest peak (FLP) and

1/2 subharmonic largest peak (SLP) are typical for the present study.

The observed features originate from the hexagonal orientation of moving VLs. In previous studies made on amorphous MoGe films,^{12–14} we have shown that the lattice orientation is characterized by whether one of close-packed (CP) directions of the hexagonal VL is parallel or perpendicular to the flow direction. For the parallel orientation, as depicted in Fig. 1a in Ref. 12, the periodic lattice spacing a in the flow direction is identified with the VL spacing, *i.e.*, $a = a_{\Delta}$, indicating the internal frequency of the moving lattice to be $f_{int} = qv/a_{\Delta}$. Since the vortex motion induces a voltage $V = lvB$ over the bridge film with length l , the voltage condition for the mode locking is given by

$$V_{p/q}^{\parallel} = \frac{p}{q} l f B_a a_{\Delta}. \quad (1)$$

We note that, in the present study, the harmonic number is always unity ($p = 1$) because of the small ac current.⁴² Assuming the lattice spacing for the regular hexagonal VL, *i.e.*, $a_{\Delta} = \sqrt{(2/\sqrt{3})\Phi_0/B_a}$ with a magnetic flux quantum $\Phi_0 (= h/2e)$, we estimate the fundamental and subharmonic ML voltages and denote them by arrows in Fig. 1b. One can see that the arrows are quantitatively in good agreement with the peaks, including the identification of harmonic p and subharmonic numbers q . Thus, from the agreements we are convinced that the FLP feature of Figs. 1a and 1b corresponds to the parallel orientation of moving lattices. The similar argument identifies the SLP feature of Figs. 1c and 1d with the perpendicular orientation of moving lattices: As sketched in Fig. 1b in Ref. 12, the perpendicular orientation is characterized by the periodicity of the row spacing $a_{\perp} [= (\sqrt{3}/2)a_{\Delta}]$ along the flow direction. Thus, the ML voltage for the perpendicular orientation is given by

$$V_{p/q}^{\perp} = \frac{p}{q} l f B_a 2a_{\perp}. \quad (2)$$

Those multiple subharmonics and fundamental are important for identifying the lattice orientation, however the conclusion does not change as long as one of identified ML features is given. To make the argument simple, we focus on the ML voltage at the largest peak of the FLP (SLP) feature.

The lattice orientation observed above depends on the vortex velocity and a flow-induced reorientation occurs as the vortex velocity (frequency) increases. This behavior can be clearly seen by showing how the ML feature changes with frequency. Figure 2a shows the results obtained in the film 2 at $B_a = 0.6$ T and $T = 2.5$ K. As depicted by open and solid square symbols, the SLP feature indicative of the perpendicular orientation appears in low frequencies, while the FLP one of the parallel orientation in high frequencies. Thus, from the ML features, one can immediately find that the flow-induced reorientation occurs at ≈ 11 MHz.

The same conclusion can be drawn from the magnitude of the ML voltage. As observed, for both features the corresponding voltage increases linearly with frequency, but there is difference in the slope related to the VL parameters. A solid line represents the ML voltage condition for the parallel orientation [Eq. (1) with $p/q = 1/1$], while a dotted line does for the perpendicular orientation [Eq. (2) with $p/q = 1/2$]. These are obtained simply by substituting the sample length l and

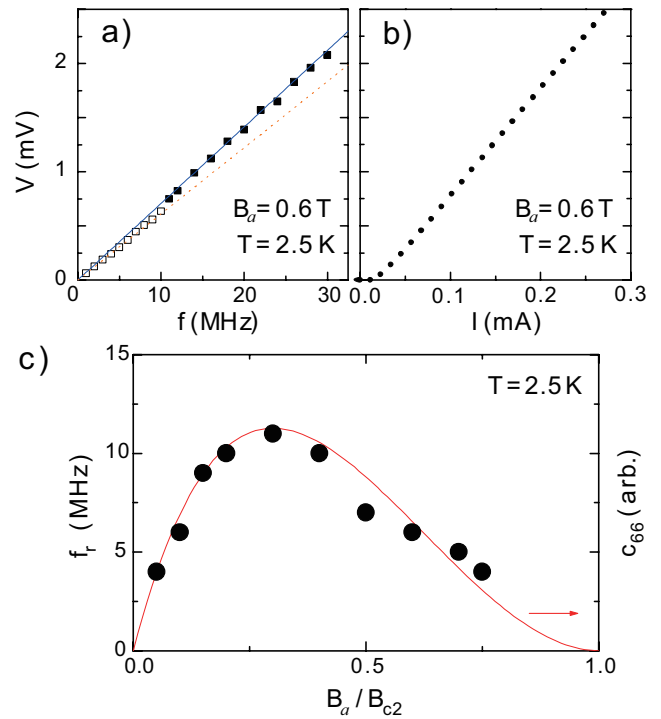


Fig. 2. (Color online) (a) ML voltage vs. frequency observed in the film 2 at 2.5 K and 0.60 T. Solid and dotted lines represent the ML conditions for parallel and perpendicular orientations, respectively. (b) The corresponding $I - V$ characteristic measured simultaneously. (c) Reorientation frequency f_r plotted against the magnetic field normalized by the second critical field $B_{c2}(2.5 \text{ K}) = 2.0$ T. A solid curve represents the field dependence of the shear elastic modulus c_{66} of the regular VL.

the magnetic field strength B_a into Eqs. (1) and (2), without adjustable parameters. One can see that the former line agrees quantitatively with the higher frequency results and the latter line does the lower frequency ones. Thus, the reorientation of moving lattices is marked by a small jump of the ML voltage at the reorientation frequency $f_r \approx 11$ MHz.

Figure 2b shows the corresponding $I - V$ curve. It exhibits the linear flux-flow behavior and does not accompany any noticeable anomaly, indicating that no discontinuous change in the vortex velocity or the vortex density occurs at the reorientation. The corresponding reorientation velocity is $v_r = f_r a_{\Delta} \approx 0.6$ m/s, which is two decades smaller than the critical velocity $v_c \sim 100$ m/s for the flux-flow instability.⁴³ These results indicate that a proposed (reorientation) mechanism based on the relaxation of the order parameter^{39,43,44} is not relevant to the observed reorientation.

Additional measurements of the reorientation made in different magnetic fields (vortex density) provide some insight into the mechanism for the reorientation. As plotted in Fig. 2c the reorientation frequency increases with the field and takes a maximum at $B_a/B_{c2} \approx 0.3$. After that, it decreases with increasing the field. The broad peak behavior of f_r is qualitatively in agreement with the field dependence of the shear elastic modulus c_{66} of the regular VL represented by a solid curve.^{30,45} This qualitative coincidence suggests that the elastic response of moving lattices plays an important role upon the flow-induced reorientation.

3.2 Moving vortex lattices in an inclined magnetic field

To track further the physical origin for the reorientation, we study how the field rotation distorts the moving lattice and also how this influences on the two orientations induced by the vortex flow. Since the London theory implies that the orientation of deformed lattices should be aligned parallelly with the tilt direction, the tilt-induced mechanism competes with the flow-induced one when the tilt- and flow- induced orientations are different. In this section, we focus on the ML results observed in two tilt directions of $\phi = 0^\circ$ and 90° , and present how the flow-induced orientation changes into the tilt-induced one as function of tilt angle θ .

Figure 3a shows the tilt dependence of the ML voltage observed in the tilt direction of $\phi \approx 90^\circ$. As denoted by open symbols, the SLP feature, indicative of the perpendicular orientation, is observed for all the tilt angles studied. This is consistent with the tilt-induced picture where one of CP directions of the hexagonal VL should be aligned parallelly with the tilt direction.³⁾ The corresponding ML voltage decreases with increasing θ , and this reduction is consistent with the dotted curve representing the ML voltage condition for $\phi \approx 90^\circ$:

$$V_{1/2}^\perp(\theta) = lfB_a a_\perp \cos \theta. \quad (3)$$

Here, we assume that the vortex density varies as $B(\theta) = B_a \cos \theta$ and the lattice parameter along the flow direction remains unchanged (Consequently, the lattice parameter along the tilt direction is stretched by $1/\cos \theta$ as illustrated in the inset to Fig. 3a). We note that the results were taken at $f = 6$ MHz ($< f_r$) and the flow-induced orientation (at $\theta \approx 0^\circ$) is the perpendicular one. Thus, the flow- and tilt-induced orientation coincide, and the perpendicular orientation appears irrespective of θ .

The situation is different at high frequencies $f > f_r$. The flow-induced, parallel orientation appears at $\theta \approx 0^\circ$ and it should switch to the tilt-induced, perpendicular orientation by rotating the field. This is clearly observed in Fig. 3b, where the ML results taken at 30 MHz ($> f_r$) are plotted. As observed, the FLP feature (the solid symbol) changes into the SLP one (the open symbol) as θ increases, and it occurs at $\theta \approx 43^\circ$. In other words, the parallel orientation persists up to $\theta \approx 43^\circ$. This is against the above picture based on the London theory that the lattice orientation should be aligned parallelly with the tilt direction at any non-zero tilt angle $\theta \neq 0^\circ$.³⁾ The corresponding ML voltages reveal how the moving lattices deform with increasing θ . The ML condition for the parallel orientation is given as

$$V_{1/1}^\parallel(\theta) = lfB_a a_\Delta \cos \theta. \quad (4)$$

This is simply $2/\sqrt{3}$ times larger than the perpendicular condition $V_{1/2}^\perp(\theta)$ in Eq. (3) since $a_\Delta = (2/\sqrt{3})a_\perp$ for the regular VL. As shown in Fig. 3b, the solid curve representing the parallel condition explains well the results until a step like drop at the reorientation angle. This quantitative agreement evidences that the moving lattices are expanded along the tilt direction. Thus, in the range of $0^\circ < \theta \leq 43^\circ$ the deformation and orientation of moving lattices do not coincide in direction as illustrated in the inset to Fig. 3b.

The discrepancy between the deformation and orientation of moving lattices also occurs in the other tilt direction of the magnetic field, *i.e.*, $\phi = 0^\circ$. Since the flow direction coincides

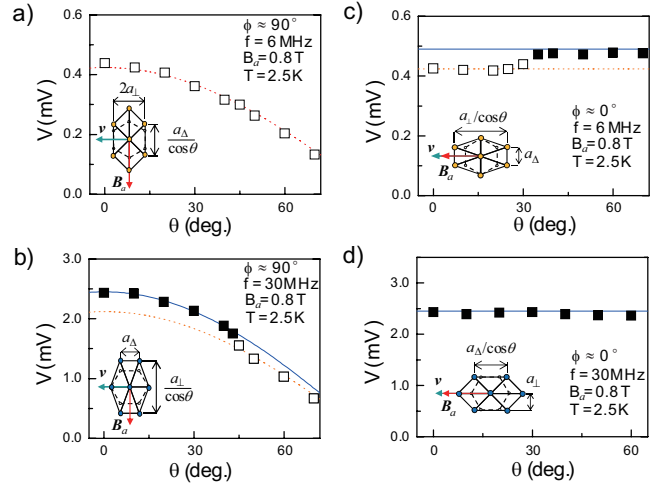


Fig. 3. (Color online) ML voltage vs. tilt angle observed in the film 2 at 2.5 K and 0.80 T. Deformed moving VLs are schematically illustrated. The flow and tilt directions are indicated by blue and red arrows, respectively.

with the tilt direction, one can expect that the deformation and orientation of moving lattices are aligned parallelly with the flow (and tilt) direction as illustrated in the inset to Fig. 3d. However, the ML features taken at the low frequency (6 MHz) reveal the presence of the perpendicular orientation at nonzero tilt angles. As shown in Fig. 3c, the perpendicular orientation persists up to $\theta \approx 30^\circ$, above which the parallel orientation appears. Thus, in the range of $0^\circ < \theta \leq 30^\circ$ the orientation of moving lattices is not aligned parallelly with the flow (and tilt) direction. The lattice deformation can be found from the tilt dependence of the corresponding ML voltage. As represented by solid and dotted lines in Fig. 3c, for both orientations the ML voltage condition is independent of θ , since the expansion of the lattice parameter along the flow (and tilt) direction by $1/\cos \theta$ (see the inset) is canceled with the reduction of the vortex density $\propto \cos \theta$. As observed, the results follow nicely the perpendicular condition (the dotted line) until $\theta = 30^\circ$, above which they do the parallel condition (the solid line). Thus, the moving lattices deform in the flow (and tilt) direction indeed, but their orientation is not aligned parallelly with the direction at low tilt angles (see the inset). Since the perpendicular orientation appears at $\theta \approx 0^\circ$, the discrepancy originates from the fact that the flow-induced orientation, being different from the tilt-induced one, survives at low tilt angles. This is not noticeable in the high frequency (30 MHz) results given in Fig. 3d where the parallel orientation appears for all the tilt angles, since the flow-induced orientation coincides with the tilt-induced one.

Let us discuss the anisotropy of VL parameters with respect to the flow direction: We define the anisotropy γ as the ratio of the lattice parameter along the flow direction divided by one perpendicular to the flow direction. Taking the perpendicular orientation of moving lattices, for instance, we obtain $\gamma^\perp(\theta) \equiv a_\perp(\theta)/a_\Delta(\theta) = a_\perp^2(\theta)B_a \cos \theta/\Phi_0 = [V_{1/2}^\perp(\theta)]^2/(l^2 f^2 \Phi_0 B_a \cos \theta)$. For the parallel orientation it needs simply to replace $V_{1/2}^\perp(\theta)$ with $V_{1/1}^\parallel(\theta)$, *i.e.*, $\gamma^\parallel(\theta) \equiv a_\Delta(\theta)/a_\perp(\theta) = [V_{1/1}^\parallel(\theta)]^2/(l^2 f^2 \Phi_0 B_a \cos \theta)$. The anisotropy thus obtained from the results in Figs. 3a ($\phi \approx 90^\circ$ and $f = 6$ MHz) and 3d ($\phi \approx 0^\circ$ and $f = 30$ MHz) is sum-

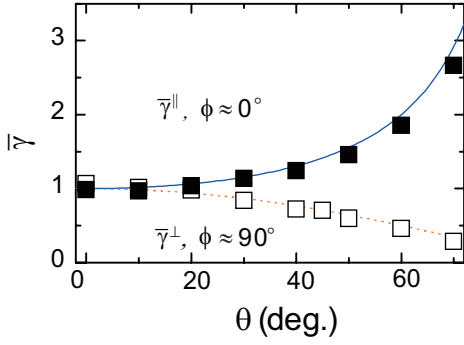


Fig. 4. (Color online) Anisotropy in the VL parameters of deformed moving VLs determined from the ML results in Figs. 3a ($\phi \approx 90^\circ$) and 3d ($\phi \approx 0^\circ$).

marized in Fig. 4. For clarity we normalize the results by the ratio of the VL parameters of the regular VL at $\theta = 0^\circ$, *i.e.*, $\bar{\gamma}^\perp(\theta) = \gamma^\perp(\theta)/(\sqrt{3}/2)$ and $\bar{\gamma}^\parallel(\theta) = \gamma^\parallel(\theta)/(2/\sqrt{3})$. One finds that $\bar{\gamma}^\perp(\theta)$ varies approximately as $\cos\theta$ represented by a dotted curve. This agrees with the picture that the moving lattices are stretched perpendicularly to the flow direction as discussed above (see the inset to Fig. 3a). Meanwhile, $\bar{\gamma}^\parallel(\theta)$ increases as $1/\cos\theta$ (represented by a solid curve) with increasing θ , being consistent with the picture of the lattice expansion along the flow direction (see the inset to Fig. 3d). These agreements give a further support for the description of lattice deformations illustrated in Fig. 3.

The above findings related to the lattice orientation imply that the tilt-induced reorientation occurs, but it depends on not only the tilt direction ϕ , but also the vortex velocity (frequency). To give further insight into the reorientation of moving lattices, it is useful to trace how the reorientation frequency f_r varies with θ . To obtain this trace, for each tilt angle θ , we measured the frequency dependence of the mode locking, and determined the reorientation frequency $f_r(\theta)$ (see Fig. 2a). The results thus obtained in the tilt direction of $\phi \approx 90^\circ$ are given in Fig. 5a. As the field is rotated, the reorientation frequency exhibits a rapid increase with downward curvature and it reaches the maximum frequency of 30 MHz at $\theta \approx 43^\circ$. Since $f_r(\theta)$ separates the parallel orientation from the perpendicular orientation of moving lattices, the results can be viewed as the dynamic phase diagram for the lattice orientation: Namely, the region of the parallel orientation lies above the $f_r(\theta)$ curve, while that of the perpendicular orientation appears below the curve. In other words, for high tilt angles ($> 43^\circ$), the tilt-induced perpendicular orientation appears irrespective of the vortex velocity. For low tilt angles ($< 43^\circ$) the lattice orientation depends on the vortex velocity and the flow-induced reorientation occurs. The corresponding reorientation velocity increases as the lattice deformation becomes larger (the anisotropy $\bar{\gamma}$ becomes smaller). Different results are obtained in the tilt direction of $\phi \approx 0^\circ$ where the moving lattices are stretched in the flow direction. As shown in Fig. 5b, $f_r(\theta)$ decreases with increasing θ and it seems to vanish at $\theta \approx 40^\circ$. Namely, for low tilt angles ($< 40^\circ$) the more stretched the moving lattices are, the smaller the reorientation frequency becomes. As a result, the region of the perpendicular orientation shrinks and the tilt-induced parallel orientation dominates high tilt angles ($> 40^\circ$). From these results we re-

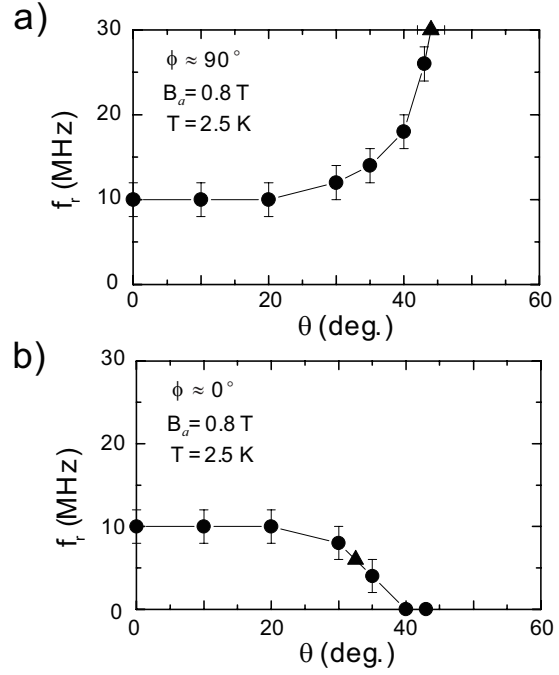


Fig. 5. Reorientation frequency vs. tilt angle (a) for $\phi \approx 90^\circ$ and (b) for $\phi \approx 0^\circ$ at 2.5 K and 0.8 T. The triangle symbols indicate the reorientation angles determined from the tilt dependences of the ML voltage given in Figs. 3b and 3c. Lines are guide to the eye.

mark that (1) for high tilt angles ($\gtrsim 40^\circ$) the field inclination determines the orientation of moving VLs: (2) For low tilt angles ($\lesssim 40^\circ$) the vortex velocity determines the lattice orientation: (3) The corresponding reorientation velocity varies sensitively as the moving lattices deform and it increases (decreases) as the anisotropy $\bar{\gamma}$ becomes small (large).

The argument of the London theory indicates that the orientation of the vortex lattice should be aligned parallelly with the tilt direction as soon as the magnetic field is tilted from normal to the film surface.³⁾ This picture disagrees with our experimental findings for low tilt angles ($\lesssim 40^\circ$). Therefore a factor(s) other than the vortex-vortex interaction should be relevant to the observed lattice orientations. Since the vortices are driven over the disordered (pinning) environment, let us discuss the above results from the viewpoint of the anisotropic shaking motion of moving lattices. Scheidl and Vinokur (SV) have introduced pinning-bond widths characterizing the relative displacements of two neighboring vortices and have argued that the anisotropy in the bond widths could determine the orientation of moving lattices.²¹⁾ When the bonds along the flow direction (x -bonds) fluctuate weakly than those perpendicular to the flow (y -bonds), the moving vortices are aligned parallelly with the flow direction. This results in the parallel orientation of moving lattices. In opposite case, the vortices should be aligned perpendicularly to the flow direction, resulting in the perpendicular orientation of moving lattices.²⁶⁾ The dependences of x - (w_x^{pin}) and y -bond widths (w_y^{pin}) on the vortex velocity v are given in limited cases:²¹⁾ For small velocities the elastic interaction dominates and both bond widths diverge as $\sim \ln(c_{66}/v)$ at $v \rightarrow 0$. However, prefactors show that the x -bond width is larger than the y -bond width. Thus their ratio $\gamma_w(\equiv w_x^{pin}/w_y^{pin})$ is more than 1 and the perpendicular orientation is favorable at small

velocities.²⁶⁾ As the velocity increases, the width of x bonds decreases as $1/v^2$, which is faster than the y bond width $\propto 1/v$, indicating the parallel orientation ($\gamma_w < 1$) at large velocities. Thus, the reorientation marks the point where the widths of x and y bonds become comparable, *i.e.*, $\gamma_w \approx 1$. We expect that this condition depends how the moving lattices deform and is scaled with the anisotropy of the lattice parameters of moving lattices, *i.e.*, $\gamma_w \approx \bar{\gamma}$. For $\phi = 90^\circ$ the condition gives $\gamma_w \approx \cos\theta (< 1)$. Namely, the x -bond width is smaller than the y -bond width, and this requires that the reorientation velocity is faster than one for no deformation at the perpendicular field ($\theta = 0^\circ$). This is consistent with our observation that f_r increases with θ (see Fig. 5a). For $\phi = 0^\circ$ the condition reads $\gamma_w \approx 1/\cos\theta (> 1)$. Namely, the x -bond width is larger than the y -bond width, and thus the reorientation velocity becomes slower. This explains qualitatively the reduction of f_r as θ increases (see Fig. 5b). A quantitative comparison can be made at the small velocity limit. According to the SV theory, the anisotropy of the bond widths is given as $\gamma_w = 1 + (\sqrt{2\pi B_a/\Phi_0\xi})/(1 + \sqrt{0.5\pi B_a/\Phi_0\xi})$. Using $B_a = 0.80$ T and the coherence length $\xi(0) = 6.9$ nm for the film 2, we obtain $\gamma_w = 1.3$. This is quantitatively consistent with the lattice expansion $\bar{\gamma} = 1/\cos\theta = 1.3$ at $\theta \approx 40^\circ$ at which f_r vanishes ($v \approx 0$). These agreements suggest strongly that the anisotropic shaking motion plays an essential role for determining the orientation of moving VLs.

A further test of the SV model can be made on confined vortex systems such as narrow constrictions^{41,46-50)} or possibly small disks.^{51,52)} The shear rigidity of moving lattices appears in the transport properties such as the flux-flow resistance, and the anisotropy in VL parameters can be tuned by the matching condition between the vortex density and the size of the constriction. These would allow systematic and quantitative investigation on how the reorientation frequency varies with the anisotropy of VL parameters in confined moving lattices.

4. Summary

In summary, we have presented ML experiments of moving VLs in amorphous NbGe superconducting films. The rf ML technique allows us to find the orientation of moving lattices as function of frequency (the vortex velocity). The flow-induced reorientation of moving lattices occurs at the characteristic frequency f_r , separating the perpendicular orientation at small velocities from the parallel orientation at large velocities. The magnetic field dependence of f_r resembles qualitatively with that of the shear elastic modulus c_{66} of the regular VL, suggesting the relevance of the elasticity of moving lattices on the reorientation.

Introducing the deformation of moving lattices by rotating the field in different directions, we have shown how the lattice orientation varies with tilt angle. The moving lattice is expanded in the direction of its motion when the field is rotated along the flow direction ($\phi \approx 0^\circ$), while for the field rotated perpendicularly to the flow direction ($\phi \approx 90^\circ$) the moving lattices are stretched perpendicularly to the flow. For high tilt angles the orientation of moving lattices is aligned parallel with the tilt direction, being consistent with the London theory. Meanwhile for low tilt angles the lattice orientation depends on the vortex velocity and the flow-induced reorientation.

we have traced how the reorientation frequency f_r varies with tilt angle. The flow-induced reorientation needs large moving velocities when the moving lattices are stretched perpendicularly to the flow direction, while it occurs at small velocities when the lattices are expanded in the flow direction. Thus, the anisotropy in VL parameters is crucial for the flow-induced reorientation. The observed features are consistent with the extended picture of the anisotropic bond fluctuation theory. This reveals that the anisotropic shaking motion is the essential mechanism which governs the orientation of moving VLs.

N. K. thanks P. H. Kes, V. M. Vinokur, M. R. Eskildsen, T. Nishizaki and S. Okuma for stimulating discussions. This work was supported partly by the grant in Aid for Scientific research from MEXT (the Ministry of Education, Culture, Sports, Science and Technology), Japan.

-
- 1) K. Takanaka: Prog. Theor. Phys. **46** (1971) 1901.
 - 2) L. J. Campbell, M. M. Doria, V. G. Kogan: Phys. Rev. **B 38** 2439 (1988).
 - 3) V. G. Kogan, L. N. Bulaevskii, P. Miranovi and L. Dobrosavljevi-Gruji: Phys. Rev. **B 51** 15344 (1995).
 - 4) C. A. Bolle, F. De La Cruz, P. L. Gammel, J. V. Waszczak, and D. J. Bishop: Phys. Rev. Lett. **71** (1993) 4039.
 - 5) H.F. Hess, C. A. Murray, and J. V. Waszczak: Phys. Rev. **B 50** (1994) 16528.
 - 6) F. Pardo, F. de la Cruz, P. L. Gammel, E. Bucher and D. J. Bishop: Nature **396** (1998) 348.
 - 7) U. Yaron, P. L. Gammel, D. A. Huse, R. N. Kleiman, C. S. Oglesby, E. Bucher, B. Batlogg, D. J. Bishop, K. Mortensen and K. N. Clausen: Nature **376** (1995) 753.
 - 8) M. R. Eskildsen: Front. Phys. **6** (2011) 398.
 - 9) A. M. Troyanovski, J. Aarts, and P. H. Kes: Nature (London) **399** (1999) 665.
 - 10) A. Kohen, T. Cren, Th. Proslie, Y. Noat, W. Sacks, D. Roditchev, F. Giubileo, F. Bobba, A. M. Cucolo, N. Zhigadlo, S. M. Kazakov, and J. Karpinski: Appl. Phys. Lett. **86** (2005) 212503.
 - 11) P. H. Kes (private communication)
 - 12) N. Kokubo, B. Shinozaki and P. H. Kes: Physica **C 468** (2008) 581.
 - 13) N. Kokubo, T. Nishizaki, B. Shinozaki and P. H. Kes: Physica **C 470** (2010) 43.
 - 14) S. Okuma, Y. Yamazaki and N. Kokubo: Phys. Rev. **B 80** (2009) 220501.
 - 15) A. Schmid and W. Hauger: J. Low. Temp. Phys. **11** (1973) 667.
 - 16) P. Le Doussal and T. Giamarchi: Phys. Rev. **B 57** (1998) 11356.
 - 17) L. Balents, M. C. Marchetti, and L. Radzihovsky: Phys. Rev. **B 57** (1998) 7705.
 - 18) C. J. Olson, C. Reichhardt, and F. Nori: Phys. Rev. Lett. **81** (1998) 3757.
 - 19) A. E. Koshelev and V. M. Vinokur: Phys. Rev. Lett. **73** (1994) 3580.
 - 20) A. B. Kolton, R. Exartier, L. F. Cugliandolo, D. Dominguez, and N. Gronbech-Jensen: Phys. Rev. Lett. **89** (2002) 227001.
 - 21) S. Scheidl and V. M. Vinokur: Phys. Rev. **B 57** (1998) 13800.
 - 22) S. O. Valenzuela: Phys. Rev. Lett. **88** (2002) 247003.
 - 23) N. Nakai, N. Hayashi, M. Machida: Physica **C 469** (2009) 1106.
 - 24) D. Li, A. M. Malkin and B. Rosenstein: Phys. Rev. **B 70** (2004) 214529.
 - 25) E. H. Brandt: Phys. Rev. **B 48** (1993) 6699.
 - 26) We note that the possibility of the perpendicular orientation at small velocities is not claimed in Ref. 21, although the analytical results of bond widths at the small velocity limit (x -bond width is larger than y -bond width) are derived.
 - 27) P. H. Kes and C. C. Tsuei: Phys. Rev. **B 28** (1983) 5126.
 - 28) N. Kokubo, K. Kadowaki and K. Takita: Phys. Rev. Lett. **95** (2005) 177005.
 - 29) A. I. Larkin and Yu. N. Ovchinnikov: J. Low Temp. Phys. **34** (1979) 409.
 - 30) P. Berghuis, and P. H. Kes: Phys. Rev. **B 47** (1993) 262.
 - 31) A. T. Fiory: Phys. Rev. **B 7** (1973) 1881.
 - 32) P. Martinoli, L. Pardi, C. Pinzino, S. Santucci: Solid State Commun. **17** (1975) 207.
 - 33) S. Bhattacharya, M. J. Higgins, and J. P. Stokes: Phys. Rev. **B 38** (1988) 7177.

- 34) T. Takayama and L. Rinderer: *J. Low. Temp. Phys.* **75** (1989) 15.
- 35) A. Maeda, Y. Togawa, H. Kitano: *Physica C* **369** (2002) 177.
- 36) T. Kawaguchi and H. Matsukawa: *Materials Science and Engineering: A* **423** (2006) 204.
- 37) A. Harada, K. Enomoto, Y. Takahide, M. Kimata, T. Yakabe, K. Kodama, H. Satsukawa, N. Kurita, S. Tsuchiya, T. Terashima, and S. Uji : *Phys. Rev. Lett.* **107** (2011) 077002.
- 38) C. Reichhardt, R. T. Scalettar, and G. T. Zimanyi: *Phys. Rev. B* **61** (2000) R11914.
- 39) S. Okuma, D. Shimamoto and N. Kokubo: *Phys. Rev. B* **85** (2012) 064508.
- 40) The magnitude of the superimposed ac current was $7\mu\text{A}$ ($< I_c \approx 20\mu\text{A}$). Meanwhile, the dc current was ramped up to ~ 1 mA in order to observe the ML feature in the flux-flow state.
- 41) N. Kokubo, R. Besseling, V. M. Vinokur and P. H. Kes: *Phys. Rev. Lett.* **88** (2002) 247004.
- 42) N. Kokubo, R. Besseling and P. H. Kes: *Phys. Rev. B* **69** (2004) 064504.
- 43) M. Liang and M. N. Kunchur: *Phys. Rev. B* **82** (2010) 144517.
- 44) D. Y. Vodolazov and F. M. Peeters: *Phys. Rev. B* **76** (2007) 014521.
- 45) E. H. Brandt: *Phys. Rev. B* **34** (1986) 6514.
- 46) A. Jukna, I. Barboy, G. Jung, A. Abrutis, X. Li, D. Wang, and Roman Sobolewski: *J. Appl. Phys.* **99** (2006) 113902.
- 47) V. Vlasko-Vlasov, U. Welp, G. Karapetrov, V. Novosad, D. Rosenmann, M. Iavarone, A. Belkin, and W.-K. Kwok: *Phys. Rev. B* **77** (2008) 134518.
- 48) A. V. Silhanek, J. Van de Vondel, A. Leo1, G. W. Ataklti, W. Gillijns and V. V. Moshchalkov: *Supercond. Sci. Technol.* **22** (2009) 034002.
- 49) K. Yu, M. B. S. Hesselberth, P. H. Kes, and B. L. T. Plourde: *Phys. Rev. B* **81** (2010) 184503.
- 50) R. Wordenweber, E. Hollmann, J. Schubert, R. Kutzner, G. Panaitov: *Physica C* **479** (2012) 69.
- 51) D. Lopez, W. K. Kwok, H. Safar, R. J. Olsson, A. M. Petrean, L. Paulius and G. W. Crabtree: *Phys. Rev. B* **82** (1999) 1277.
- 52) N. S. Lin, V. R. Misko, and F. M. Peeters: *Phys. Rev. Lett.* **102** (2009) 197003.